Quasi-geostrophic modelling of the coupled ocean atmosphere

John A. T. Bye, The Flinders University of South Australia, Adelaide, Australia
and
Jörg-Olaf Wolff, Antarctic CRC, Hobart, Australia

Abstract The momentum balance of the Antarctic Circumpolar Current is a fundamental problem in oceanography. In a series of solutions of a fine resolution quasi-geostrophic model coupled to the atmosphere by a surface stress relation we show that the response to a fluctuating wind stress in an Antarctic channel is 70% efficient, and generates almost frictionless transport oscillations. The application of the analysis to scatterometer wind data in the Antarctic Channel indicates that the effective lag of the transport over the wind fluctuation is about 10 days in agreement with observations.

1 Introduction

The exchange of momentum at the sea surface occurs on all time scales. In this paper we consider this process over periods greater than synoptic, but less than seasonal. The variability of the local surface stress over this frequency band has been investigated recently for the Circumpolar Channel from scatterometer data (Madden, 1997), and the results obtained in this modelling study can be used to predict the resultant variability in the transport of the Antarctic Circumpolar Current.

2 The model

The model which is used is the fine resolution two-layer quasi-geostrophic model originally developed by Wolff et al. (1991), with the surface stress coupling introduced by Wolff and Bye (1996) in which the surface shear stress,

$$\vec{\tau} = \rho_1 K_I \left|\vec{u}_1 - \frac{1}{\epsilon}\vec{u}_2\right| \left(\vec{u}_1 - \frac{1}{\epsilon}\vec{u}_2\right) \qquad (1)$$

where ρ_1 is the density of air, $\epsilon = \sqrt{(\rho_1/\rho_2)}$ in which ρ_2 is the density of water (in the upper layer), $\vec{u}_1$ is the air velocity, and $\vec{u}_2$ is the water velocity in the upper layer, and K_I is a drag coefficient. An important feature of this relation is that $\vec{\tau}$ is the surface shear stress in the Earth reference frame, rather than that observed in a local reference frame in which planetary boundary layer measurements including scatterometer measurements are made. It is found that a realistic momentum balance in the Antarctic channel could be obtained using form drag and the surface stress coupling (1) without the need to involve a large (unrealistic) braking by bottom friction. The direct application of (1) with a steady zonal wind generated almost steady solutions in which the streamline pattern was similar to the mean streamfield of the corresponding eddy-resolving solutions (Bye and Wolff, 1997).

In this study we consider a local zonal wind stress of the form,

$$\tau_s(x,t) = \left(\tau_1 + \tau_2 \sin\frac{2\pi t}{T_o}\right)\sin\frac{\pi y}{Y} \qquad (2)$$

where τ_1 and τ_2 are constant stresses, T_o is the period of the harmonic oscillation and Y is the channel width. The results obtained for the harmonic fluctuations allow the transport variability produced by the time series,

$$\tau_s(x,y) = \tau_3(t)\sin\frac{\pi y}{Y} \qquad (3)$$

where $\tau_3(t)$ is obtained from scatterometer data, to be assessed. In all the solutions the momentum balance in the channel is represented by the equation,

$$\frac{\partial}{\partial t}T = \int_0^Y <\tau> dy + \int_0^Y < B\frac{\partial p}{\partial x} > dy \qquad (4)$$

in which T is the transport, τ is the zonal component of the surface shear stress, $B\partial p/\partial x$ is the form drag in which p is the pressure in the lower layer, $B(x,y)$ is the topographic height (in the lower layer), and $< \cdot >$ denotes a zonal average. Equation (4), which is derived in Wolff et al. (1991), indicates that changes in transport are produced by the net effect of the surface stress and the bottom drag. The surface wind ($\vec{u}_1$) in (1) is obtained from the relations,

$$\tau_s = \rho_1 K_I u_1^2 \qquad (5)$$

and $v_1 = 0$ in which τ_s is given by (2).

The model parameters are the following: upper layer depth (H_1 = 1 km), lower layer depth (H_2 = 4 km), mesh interval ($\Delta x = \Delta y$ = 20 km), time step (Δt = 2 hours), reduced gravity (g' = 0.02 ms^{-2}), density of water (ρ_2 = 1000 kgm^{-3}), density of air (ρ_1 = 1.2 kgm^{-3}), and drag coefficient ($K_f = 1.2 \cdot 10^{-3}$). The solution is obtained in an annulus of length (X = 4000 km) and width (Y = 1500 km) in which a cyclic topography based on the Macquarie Ridge Complex is implemented in the lower layer (Wolff et al. 1991).

3 Results

3.1 Steady wind forcing

The evolution of the transports for steady wind forcing, τ_1 = 0.1 Nm^{-2} and τ_2 = 0, over a run of approximately 600 years is shown in Fig. 1.

The time mean transports are 122 Sv (1 Sv = 10^6m^{3}s^{-1}) in the upper layer, and 66 Sv in the lower layer (see Table 2), which indicates a strongly baroclinic response. There is also a natural variability in each transport typically of period of a few months, and of range 15 Sv (lower layer) and 4 Sv (upper layer). The time mean streamfields (Fig. 2) indicate a well formed central jet in the upper layer, and the tendency for the formation of closed topographically induced eddies in the lower layer. Fig 3 shows the time series of the terms in the momentum balance equation (4) over the final $10^4\Delta t$ (833 days) of the run. The steady-state balance is between the surface stress and the form drag which each are of magnitude of about 50 m^{3}s^{-2}. The corresponding channel integral of the wind stress,

$$\int_0^Y < \tau_s > dy = \frac{2Y}{\pi}\tau_1 \qquad (6)$$

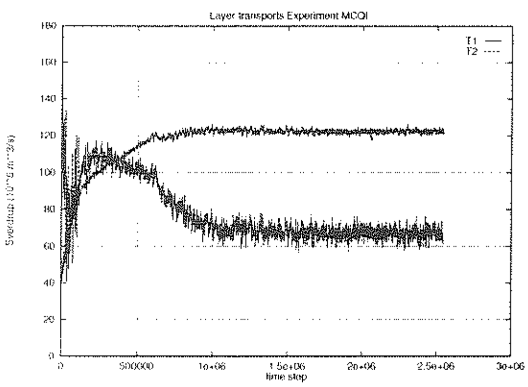

Figure 1: Time evolution of volume transports in the upper layer (T_1) and the lower layer (T_2) for steady wind forcing, Transport in units of Sv (1 Sv = 10^6m^{3}s^{-1}), time axis in units of time steps Δt ($1\Delta t$ = 2 hr), from Bye and Wolff (1997).

T_0	$\frac{\partial T}{\partial t}$	$\int\langle\tau\rangle dy$	$\int\langle B\frac{\partial p}{\partial x}\rangle dy$	$\int\langle\tau_s\rangle dy$
days	m^{3}s^{-2}			
6	23	23	0	33
15	28	22	6	33
∞	0	50	-50	95

Table 1. Momentum balance in the Antarctic channel (terms are defined in (4) and (6)). The entries show the time mean amplitude of the terms for the period T_o, the infinite period refers to the steady state solution.

has a magnitude of 95 m^{3}s^{-2} (see Table 1). Hence in the steady-state, approximately 1/2 the wind stress is returned to the atmosphere, and the other 1/2 is dissipated by form drag.

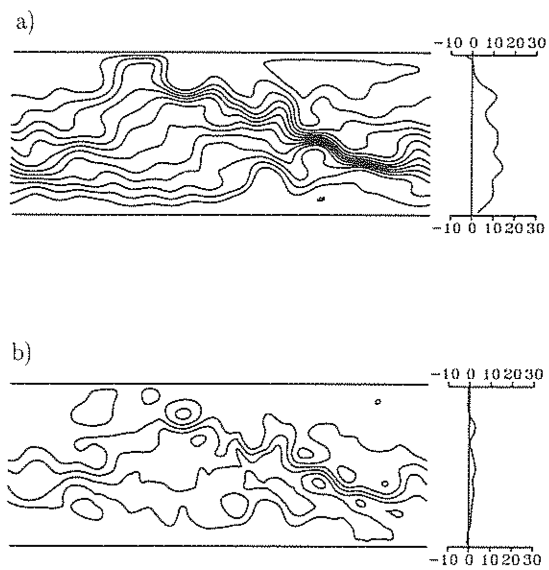

Figure 2: Time mean streamfunctions of experiment MCQI, a) upper layer CI = 10^4 m^{2}s^{-1} and b) lower layer CI = $5 \cdot 10^3$ m^{2}s^{-1}. The zonally averaged time-mean velocity as a function of latitude is indicated to the right of each panel. Units cm/s. (from Bye and Wolff, 1997).

3.2 Harmonic stress forcing

Two periods (T_o = 6 days and T_o = 15 days) were considered, with τ_1 = 0.1 Nm^{-2} and τ_2 = 0.035 Nm^{-2}. Fig 4 shows that the total transport variability associated with the steady wind persists, on which is superimposed the harmonic signal due to the surface stress fluctuation. For the 6 day period, the amplitude of the oscillation is about 2 Sv. The

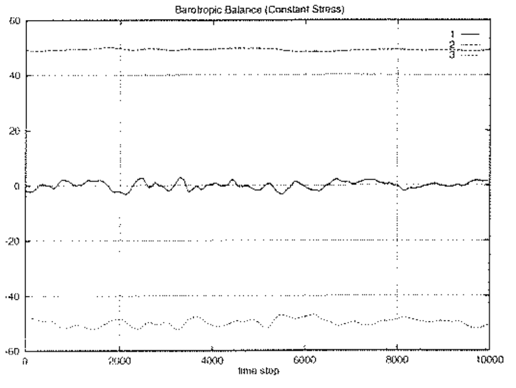

Figure 3: Segment (10000 Δt) of time evolution of the momentum balance in the Antarctic Channel for steady wind forcing; (1) $-\partial T/\partial t$, (2) $\int_0^Y <\tau> dy$ and (3) $\int_0^Y <B\partial p/\partial x> dy$.

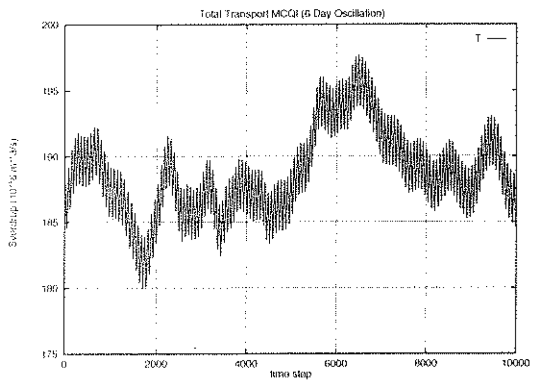

Figure 4: Time evolution of volume transport (T) for a fluctuating wind stress comprising a steady wind and a six day oscillation for a 10000 Δt segment.

balance of terms in (4), which maintain the transport oscillation over a period of $10^3\Delta t$ shows that the fluctuating surface stress maintains the oscillation without any significant contribution from form drag (Fig. 5) and Table 1 indicates that about 70% of the fluctuating wind stress is transmitted to the ocean. It is also apparent that $\partial T/\partial t$ and τ are very nearly in phase, indicating that the oscillation is almost frictionless. The corresponding time series (Fig 6) for the 15 days oscillation, shows that the form drag is not negligible, and that the amplitude of the 15 day transport oscillation is much greater than for the 6 day transport oscillation. It is also apparent that all the terms in (4) are approximately in phase, and hence the form drag augments the surface stress in maintaining the oscillation, which is an unexpected result. Nevertheless, a very similar proportion (~ 0.7) of the wind stress is available to the ocean as for the 6 day oscillation (Table 1). The proportions of the oscillatory transport occurring in the upper and lower layers (Table 2) indicate that the response is almost barotropic at both periods, with a slightly reduced relative lower layer transport (90-95% of barotropic). This is in contrast to the steady solution in which the lower layer transport is only about 1/7 of the barotropic value.

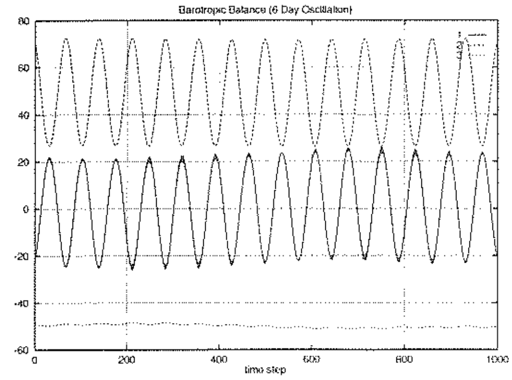

Figure 5: Segment (1000 Δt) of time evolution of the momentum balance for a steady wind with a six day oscillation; (1) $-\partial T/\partial t$, (2) $\int_0^Y <\tau> dy$ and (3) $\int_0^Y <B\partial p/\partial x> dy$.

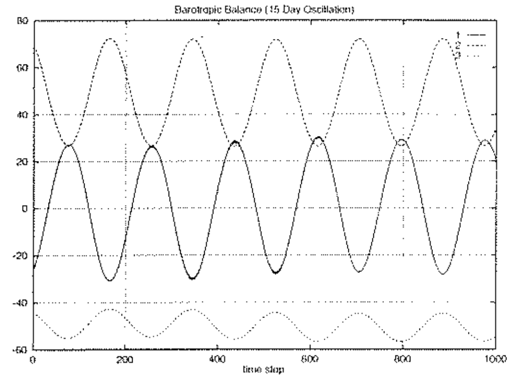

Figure 6: Segment (1000 Δt) of time evolution of the momentum balance for a steady wind with a fifteen day oscillation; (1) $-\partial T/\partial t$, (2) $\int_0^Y <\tau> dy$ and (3) $\int_0^Y <B\partial p/\partial x> dy$.

3.3 The high frequency limit

These results allow the following simple analytical model to be constructed for the high frequency limit of the oscillatory motion. Since at high frequencies ($T_o \longrightarrow 0$) the amplitude of the transport and also of the oscillatory current in the lower layer become negligible, (4) reduces to the relation,

$$\frac{\partial T}{\partial t} = \int_0^Y <\tau_1'> dy \qquad (7)$$

where τ_1' is the surface stress due to the wind fluctuation. In this limit, the surface stress reduces to the expression,

$$\vec{\tau} = \rho_1 K_I \left|\overline{\vec{u}}_1 - \frac{1}{\epsilon}\overline{\vec{u}}_2 + \vec{u}_1'\right| \left(\overline{\vec{u}}_1 - \frac{1}{\epsilon}\overline{\vec{u}}_2 + \vec{u}_1'\right) \qquad (8)$$

in which the overbar and the prime denote respectively a mean and fluctuation, and $u_2' = 0$. On now

T_0	T_1	T_2
days	Sv	
6	0.4	1.5
15	1.2	4.6
∞	122	66

Table 2. Transport amplitudes in the Antarctic channel (T_1 and T_2 are upper and lower layer transports, respectively). The entries show the time mean amplitude of the terms for the period T_o, the infinite period refers to the steady state solution.

making the three approximations: (i) zonal velocities are much greater than meridional velocities, (ii) the wind velocity fluctuation (u_1') is much less than the mean wind ($\overline{u}_1$), and (iii) the steady state transport momentum balance can be applied uniformly across the channel such that,

$$\overline{u}_1 - \frac{1}{\epsilon}\overline{\overline{u}}_2 = \alpha\overline{\overline{u}}_1 \qquad (9)$$

where $\overline{\overline{u}}_2$ is the mean current in the upper layer, and α is a constant, we obtain,

$$\tau \approx \rho_1 K_J \left(\alpha^2\overline{\overline{u}}_1^2 + 2\alpha\overline{u}_1'\overline{\overline{u}}_1\right) \qquad (10)$$

from which the integral of the fluctuating stress,

$$\int_0^Y < \tau' > dy = \frac{2Y}{\pi}\left(\alpha\tau_2 \sin\frac{2\pi t}{T_o}\right) \qquad (11)$$

and hence

$$T = A\sin\left(\frac{2\pi t}{T_o} - \frac{\pi}{2}\right) \qquad (12)$$

where

$$A = \frac{T_o Y \alpha}{\pi^2}\tau_2 \qquad (13)$$

Equation (11) indicates that a fraction (α) of the wind stress is available to drive the transport oscillation, and (13) is an explicit expression for the amplitude of the transport oscillation. The steady-state solution (Table 1) indicates that $\alpha \sim 0.7$, and on substituting for α in (13) for $T_o = 6$ days, we obtain, $A = 1.9$ Sv. Both these estimates are in good agreement with the computed results (Table 2). In summary, the analytical model predicts a $(T_o\alpha)^2$ weighting of the local surface stress spectrum as $T_o \longrightarrow 0$ (which is approximately valid over the energetic range of the scatterometer spectrum), and also that the transport variations lag the wind fluctuations by $\pi/2$ as would occur in a frictionless system.

4 Application to the scatterometer data

The high frequency limit of Section 3.3 has been used to obtain preliminary results on the transport response of the Antarctic Circumpolar Current to the variable wind stress field determined from scatterometer data.

The procedure was to digitize the $50^o - 60^o$S zonally averaged scatterometer wind for the period January-March 1992, shown in Fig. 2 of Madden (1997) at a daily interval. From the resulting time series of 90 wind values, the wind fluctuation (u_1') was obtained and resolved into a Fourier series of harmonics, which were used to determine T from (12). Finally the lagged correlation of the time series T relative to u_1' was obtained.

It is found that the correlation coefficient ($r_{\tau T}$) has a broad maximum ($r_{\tau T} \sim 0.3$) centered around a lag of about 10 days (Fig. 7). This is due to the shape of the energy spectrum of the fluctuating wind. The correlation coefficient becomes zero at a lag of about 30 days, and is necessarily zero at zero lag, cf (12).

These results are in good agreement with observations of meridional bottom pressure gradients and wind stress from the study of Wearn and Baker (1980) in which a lag of 9 days, and also a maximum correlation of coefficient of 0.3 with respect to the local wind stress, were obtained.

The lagged autocorrelation coefficient (r_{TT}) for the synthetic transport variability was also computed and found to have a first zero between 18 and 19 days (Fig. 7). This prediction is in good agreement with current meter observations in the Drake Passage, from which determination of the autocorrelation coefficients indicated a first zero at a mean of 14 days, and a range of 6-32 days (Bryden and Pillsbury 1977).

These comparisons suggest that the quasi-geo-

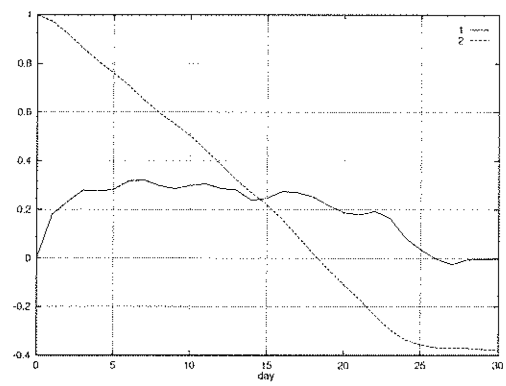

Figure 7: Lagged correlation coefficients, $r_{\tau T}$ (1, solid line) and r_{TT} (2, dashed line).

strophic solutions with surface stress coupling are a good model for the non-divergent time-dependent response of the Antarctic Circumpolar Current, however detailed comparison using the scatterometer wind data is necessary for a proper assessment.

5 Conclusion

Solutions of a two-layer quasi-geostrophic model, forced by a fluctuating wind stress, coupled to the ocean by the surface stress relation (1) (which takes account of the surface wave field) generate a transport spectrum in the Antarctic Circumpolar Channel, in which about 70% of the wind stress is transmitted to the ocean. On applying this momentum balance to the observed scatterometer wind it is found that the effective lag of the transport over the wind is about 10 days in agreement with observations. This preliminary study suggests that Ocean General Circulation Models can be used to predict the transport variability of the Antarctic Circumpolar Current accurately using the surface stress relation (1).

6 References

Bryden, H.L. and R.D. Pillsbury. Variability of deep flow in the Drake Passage from year long current measurements. *J. Phys. Oceanogr.*, 7(6), 803-810, 1977.

Bye, J.A.T. and J.-O. Wolff. On atmosphere-ocean momentum exchange in general circulation models. *J. Phys. Oceanogr.*, (submitted). 1997.

Madden, R.A. The variability of surface winds in the vicinity of the Antarctic Circumpolar Current Fifth Intl Conf in Southern Hemisphere Meteorology and Oceanography Preprint Volume Amer. Met. Soc., 188-189, 1997.

Wearn, R.B. and D.J. Baker. Bottom pressure measurements across the Antarctic Circumpolar Current and their relation to wind. *Deep Sea Res.*, 27A 875-888, 1980.

Wolff, J.-O. and J.A.T. Bye. Inertial surface stress coupling in a two-layer quasi-geostrophic model. *Ocean Modelling*, 112, 6-8, 1996.

Wolff, J.-O., E. Maier-Reimer and D.J. Olbers. Wind-driven flow over topography in a zonal $\beta-$plane channel : A quasi-geostrophic model of the Antarctic Circumpolar Current. *J. Phys. Oceanogr.*, 21(2), 236-264, 1991.